ACTA ASTRONOMICA
Vol. **62** (2011) pp. 0–0

Open clusters in 2MASS photometry – I. Structural and basic astrophysical parameters

Ł. Bukowiecki, G. Maciejewski, P. Konorski and A. Strobel

Toruń Centre for Astronomy, Nicolaus Copernicus University, Gagarina 11, PL-87-100 Toruń, Poland
e-mail: bukowiecki@astri.umk.pl

Received June 5, 2011

ABSTRACT

The main goal of our project is to obtain a complete picture of individual open clusters from homogeneous data and then search for correlations between their astrophysical parameters. The near–infrared JHK_S photometric data from the 2–Micron All Sky Survey were used to determine new coordinates of the centres, angular sizes and radial density profiles for 849 open clusters in the Milky Way. Additionally, age, reddening, distance, and linear sizes were also derived for 754 of them. For **these** open clusters our results are in satisfactory agreement with the literature data. The analysed sample contains open clusters with ages in the range from 7 Myr to 10 Gyr. The majority of these clusters are located up to 3 kpc from the Sun, less than 0.4 kpc from the Galactic Plane and 6 – 12 kpc from the Galactic Centre. The majority of clusters have core radii of about 1.5 pc and the limiting radii of the order of 10 pc. We notice that in the near–infrared, open clusters seem to be greater than in optical bands. We notice that a paucity of clusters is observed at Galactic longitudes range from 140° to 200° which probably reflects the real spatial distribution of open clusters in the Galaxy. The lack of clusters was also found in earlier studies.

Key words:

open clusters and associations: general – infrared: galaxies – astronomical databases: 2MASS

1. Introduction

In this paper the near-infrared JHK_S photometric data were used to redetermine equatorial and galactic coordinates of the centres of known open clusters. This allowed us to construct radial density profiles of clusters and to determine their core radii and estimate their limiting radii. The adopted background-star decontaminating procedure allowed us to construct colour–magnitude diagrams for individual clusters and to estimate ages for a significant fraction of the considered sample.

The structure of this paper is as follows. In Section 2 the method and data analysis is presented. In Section 3 our results are compared to the results found in

literature. Section 4 contains discussion of the relations between individual parameters. Final conclusions are summarized in Section 5.

Similar to our research, Janes (1979) used UBV photometry to study the reddening and metallicity of 41 open clusters. Comparison between the age and position in the Galaxy was studied by Lyngå (1980, 1982). Janes & Phelps (1994) based on 72 open clusters and Friel (1995) with a sample of 74 objects investigated how the extinction and age depend on a position in the Galaxy. Tadross et al. (2002) and Schilbach et al. (2006) studied how open clusters diameters and age depend on position in the Galactic Plane. Previous research of open clusters in 2MASS photometry were done by Dutra & Bica (2001) who studied 42 new infrared star clusters, stellar groups and candidates towards the Cyngus X region. Bica et al. (2003) based on 2MASS researched 346 open clusters, whereas 315 objects were previously known. They studied linear diameters and spatial distribution of open clusters in the Galaxy. Recently Froebrich et al. (2010) studied 269 open clusters and the age, core radius, the reddening, Galactocentric distance and the scaleheight were determined.

2. Data analysis

2.1. Data source and selection of clusters

The list of open clusters and their initial central coordinates were taken from the compilation *New catalog of optically visible open clusters and candidates* by Dias et al. (2002). Our research is based on the JHK_S photometric data extracted from the 2MASS[1] *Point Source Catalog* (Skrutskie et al. 2006). The adopted extraction radius for each listed cluster was equal to 30 + 4 arcmin, because we wanted to focus on well defined, concentrated open clusters of angular diameters smaller than 60 arcmin. The additional 4 arcmin were added as a margin for cases in which the true centres were found at different location. This step resulted in a collection of 1756 catalogue fields.

The next step was to identify the star cluster in each of extracted field. In many cases this task was not trivial because some clusters were found to be poor, sometimes consisting of only from a few to several dozen members, and sparse due to a significant angular size. Moreover, the stellar background in near IR is relatively high, making the identification of a cluster very uncertain or even impossible. In some cases, it was necessary to exclude open clusters from further consideration as they were too wide or not rich enough for reliable analysis. Finally, after a visual inspection of pictures from the 2MASS and iterative construction of radial density profiles (RDP) for 1756 clusters, we limited our sample to 849 unambiguously identified objects (see Sect. 2.2 and 2.3) for which reliable centre coordinates could be determined.

[1] http://www.ipac.caltech.edu/2mass/releases/allsky/

2.2. Central coordinates

Visual inspection of the extracted fields suggested that for the majority of open clusters their catalogue coordinates were much different from the real ones. Hence, they must have been redetermined. The algorithm for determination of the cluster centre was adopted from Maciejewski and Niedzielski (2007). The procedure starts with initial coordinates of cluster centres taken from the catalogue by Dias et al. (2002). In some cases, the discrepancies were so significant that it was necessary to define the initial coordinates by hand as a result of visual inspection. In the considered field, the algorithm cuts off two perpendicular rectangular stripes along declination and right ascension, crossed over an approximated cluster centre, and a histogram of star counts is built along each stripe. The length and width of those stripes are chosen individually for each cluster and depend on its size. Typically, the length ranges from 5 to 30 arcmin and the width from 1 to 8 arcmin. Bins with the positions of the maximum value in both coordinates indicate a new cluster central coordinates. This procedure was repeated iteratively until the new position of the cluster centre converged into a stable point on the sky.

2.3. Angular sizes

To study the cluster structure, a radial density profile was constructed for each cluster by star counts inside concentric rings centred at the redetermined centre coordinates. The observed stellar density ρ was calculated for each ring and plotted as a function of the angular radial distance from the cluster centre. Then, this density distribution was parametrised by a two-parameter King-like function (King 1966):

$$\rho(r) = f_{bg} + \frac{f_0}{1 + \left(\frac{r}{r_{core}}\right)^2}, \tag{1}$$

where r_{core}, f_0, and f_{bg} are the core radius, the central density, and the background density level, respectively. The core radius was defined as a distance where the stellar density drops to half of f_0. These parameters were determined by the least-square method. The cluster limiting radius, r_{lim}, was calculated by comparing $\rho(r)$ to a border background density level, ρ_b, defined as:

$$\rho_b = f_{bg} + 3\sigma_{bg}, \tag{2}$$

where σ_{bg} is uncertainty of f_{bg}. Finally , r_{lim} was calculated according to the following formula:

$$r_{lim} = r_{core}\sqrt{\frac{f_0}{3\sigma_{bg}} - 1}. \tag{3}$$

The widths of concentric rings were set equal to uncertainties (errors) of r_{lim} and ranged from 0.14 to 4.4 arcmin, depending on **the** angular diameter of each cluster and stellar crowding. They were further refined individually for each object

to obtain the RDP as smooth as possible. We combined both r_{core} and r_{lim} in a form of the concentration parameter $c = \log(r_{lim}/r_{core})$ (Peterson and King 1975) to characterise the structure of clusters. The structural parameters – new equatorial and galactic coordinates and angular sizes of all object in the sample – are given in Table 1 in Appendix A.

2.4. The colour–magnitude diagram analysis

Analysis of colour–magnitude diagrams (CMDs) is a commonly used method to derive age, reddening, and distance – the most fundamental parameters characterising stellar clusters. For each cluster of our sample, a J *vs.* $(J-K_S)$ colour–magnitude diagram was constructed. Although in general it is impossible to point out individual cluster members without additional information, *e.g.*, proper motion, the contribution from field stars can be removed from the cluster CMD in a statistical sense. The algorithm applied to our data was based on the idea , presented in Mighell et al. (1996) and discussed in Bica and Bonatto (2005), of statistical subtracting a CMD of a background field outside of the cluster area from a CMD of a field occupied by a cluster. Because of various contrast of individual clusters against the Galaxy background, the boundary of the area occupied by a cluster was chosen individually for each cluster as a result of iterative tests. In practice values between 1 and 4 r_{core} were used, depending on a ratio r_{lim}/r_{core} (based on our calculations). When this ratio was greater than 9 we used 3-4 r_{core}, when was less than 5.5 we used 1-2 r_{core}, for other cases we used 2-3 r_{core} (exact values of r_{core} are listed in Table 1 in Appendix A). A concentric offset field began at $r = r_{lim} + 1$ arcmin from the cluster centre and usually ended at 34 arcmin. Both CMDs were divided into two–dimensional bins of $\Delta J = 0.4$ mag and $\Delta(J-K_S) = 0.1$ mag size (both values being fixed after a series of tests, as a compromise between resolution and the star numbers in individual boxes). The number of stars within each box was counted. The cleaned (decontaminated) CMD was built by subtracting a number of stars in an offset box from a number of stars in a corresponding cluster box. The latter number was weighted by the cluster–to–offset field area ratio. According to this procedure the algorithm randomly chose the required number of stars located in the cluster area and with the adequate magnitude and colour index. Finally, the list of stars in each cleaned cluster box was saved and used for constructing the decontaminated CMD.

After applying the CDM cleaning procedure, we limited our sample to 754 open clusters with well visible main sequence and red giant clump (excluding very young clusters). Stars which were found to be outliers from main sequence and red giant clump were removed by hand in a result of visual inspection. Finally, the distances moduli, reddenings, and ages were derived by fitting the Padova isochrones at J *vs.* $J-K_S$ bands for solar metallicity $Z = 0.019$ (Girardi et al. 2002) to the decontaminated CMDs. The isochrones cover a wide range of ages from 4 Myr up to 14 Gyr with a step of 0.05 in the logarithm of age. Theoretical isochrones

were shifted in both directions in the CMDs with a step of 0.01 mag. The solution giving the smallest χ^2 was taken as a final one. In a series of tests we checked how the reddening and distance modulus determination depend on choosing different angular sizes of both cluster and offset–field areas. We found that the spread of results, represented by the standard deviation, usually did not exceed 0.03 and 0.10 mag, for the reddening and distance modulus, respectively. **Step of 0.05 in the logarithm of age** was adopted as a typical uncertainty of the log(*age*) but for younger clusters for which we could not detect giant stars and we used only ZAMS stars, the individual error can be greater. In these cases our values of age are more like "not older than". **We present six CDMs for open clusters with different age in Appendix B.**

Results from the analysis of CMDs allowed us to calculate cluster distances from the Sun and transform angular sizes into linear ones. The determined astrophysical fundamental parameters are listed in Table 2 in Appendix A.

3. Comparison with the published data

To test a reliability of our determination, we compared our results with the literature data. We took them from the open cluster catalogue by Dias et al. (2002) or from papers dedicated to individual clusters, if available. Fig. 1a presents comparison of angular limiting radii obtained by us in the near IR with data in visual bands from the literature for 337 open clusters. Fig. 1b presents the same comparison but for angular core radii and for 85 objects. As it can be easily seen, for the majority of observed open clusters our calculations of angular sizes (near IR) appear to be even several times larger than the catalogue records indicate. This has already been noticed by Sharma et al. (2006). This effect seems to be particularly distinct for small – according to catalogue data – objects, for which our estimations of this parameter appear to be up to six times greater. **This** effect may be a result of missing faint cluster members in many photometric studies **which are** based on optical photometry, partly due to significant influence of the interstellar extinction or using the field of view not wide enough. Using the 2MASS survey allows us to avoid both of these limits: provide wide cluster fields coverage with homogenous data and minimise the interstellar absorption in the infrared.

We expected that ages of open clusters determined by us will be very close to the literature ones because the use of data from different photometric bands should have little influence on determining this parameter. In our sample we found 536 open clusters with known ages. In Fig. 2a our results are plotted against the published values. The majority of points is located near a straight line corresponding to a perfect match. Thirteen outlying points, marked as **triangles**, were rejected during fitting a linear relation. We obtained:

$$log\,(age)_{our} = (1.05 \pm 0.06)\, log\,(age)_{lit} \qquad (4)$$

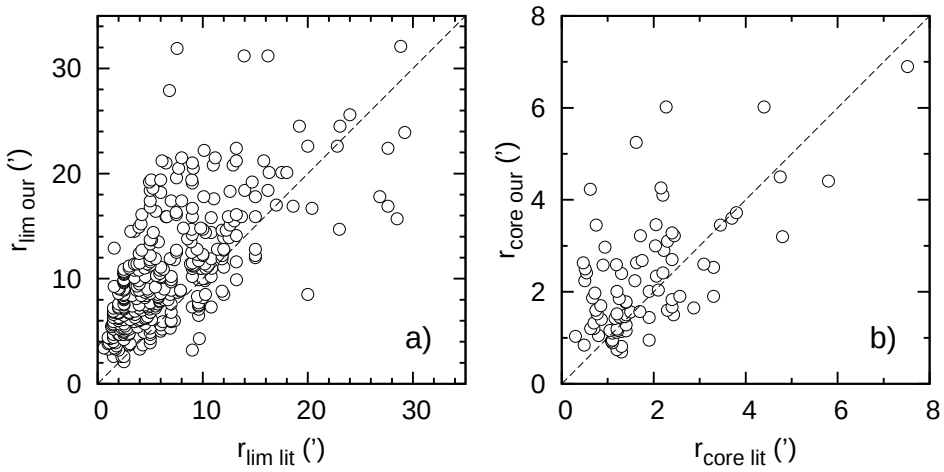

Fig. 1. a) A comparison of angular limiting radii obtained by us in near-IR (JHK) and the literature data obtained in visual bands (UBV) for 337 open clusters. The dotted line shows a case of perfect match, i.e. $y = x$. b) The same as panel a but for angular core radii for 85 clusters.

with the correlation coefficient of 0.96.

To calculate the interstellar reddening $E(B-V)$, we adopted the interstellar extinction law by Schlegel et al. (1998) **and Bessell (2005)** $\boldsymbol{E(J-K_S) = 0.972\ E(J-K)}$ **assuming** $\boldsymbol{E(J-K_S)/E(B-V) = 0.520 \pm 0.045}$. In Fig. 2b we plot the comparison of the obtained colour excess $E(B-V)$ with the literature data for 543 clusters. Twenty nine outlying clusters, which were found to be located too far from the main trend, were not taken into account during fitting procedure. We obtained a linear relation:

$$E(B-V)_{our} = (\mathbf{0.89} \pm 0.01)\, E(B-V)_{lit} \tag{5}$$

with the correlation coefficient equal to **0.91**. Our determinations were found to be somewhat lowered comparing to the published ones. This suggests slightly different ratio $E(J-K_S)/E(B-V) = \mathbf{0.463}$.

We calculated distances to the clusters assuming relations $E(J-K_S)/E(B-V) = \mathbf{0.520}$ and $A_J/A_V = 0.276$ and under the assumption of the total-to-selective absorption ratio of $R = 3.1$ (Cardelli et al. 1989). In Fig. 2c the distances, d, are plotted against published data for 532 objects. Almost all points are located along a diagonal line corresponding to a perfect match. After removing thirteen outlying objects, we obtained a linear relation:

$$d_{our} = (0.97 \pm 0.09)\, d_{lit} \tag{6}$$

resulting in the correlation coefficient of 0.93. This result allows us to find our

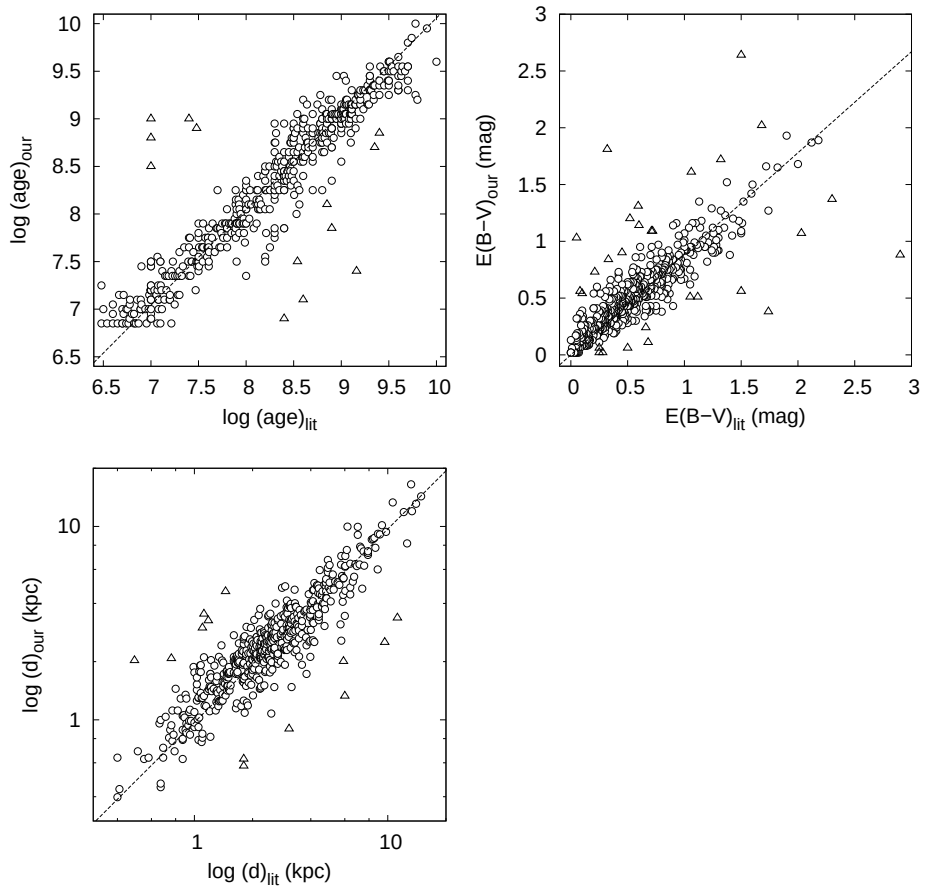

Fig. 2. a) Open clusters ages derived by us as a function of the literature data. The best–fitting linear relation of a the form $y = ax$ is marked with a dashed line. **Triangles** were rejected during fitting a linear trend, see text for details. b) The same as panel a but for the interstellar reddening $E(B-V)$. c) The same as panel a but for the distance from the Sun d.

determinations of d reliable. It is worth noticing that adopting the relation $E(J-K_S)/E(B-V) = \mathbf{0.463}$ would change d only by **2.8**% – a value two times smaller than typical errors based on the distance modulus.

4. Discussion of statistical relations between parameters

4.1. Reddening, age, radial structure and distribution in the Galactic Plane

Structural and physical parameters determined for statistically significant number of open clusters allowed us to check mutual relations between individual parameters. Fig. 3a) presents a relation between the interstellar reddening ($E(B-V)$) and a distance from the Galactic Plane (Z). The presented relation indicates that

for objects located within $Z = \pm 0.1$ kpc the average reddening is equal to **0.68** mag and decreases with increasing $|Z|$. For clusters with $|Z|$ between 0.1 and 0.4 kpc the mean $E(B-V)$ is equal to **0.51** mag and drops to **0.34** mag for $|Z| > 0.4$ kpc. We performed similar statistical analysis for a distribution of $E(B-V)$ along cluster distances from the Galactic Centre, R_{GC} (Fig. 3b). The mean $E(B-V)$ for open clusters located near the Sun (8.3 kpc) and far beyond the Galactic orbit of the Sun is **0.74** and **0.53** mag, respectively. Both trends **were noticed by Janes & Phelps (1994)**.

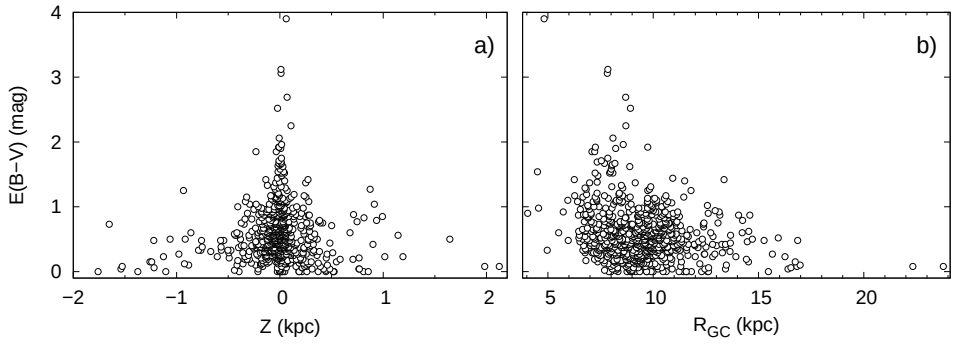

Fig. 3. *Left*: The relation between the reddening $E(B-V)$ and distance from the Galactic Plane Z assuming $Z_{\odot} = -33$pc. *Right:* Relations between the reddening $E(B-V)$ and distance from the Galactic Centre R_{GC}, assuming $R_{GC\odot} = 8.3$kpc.

Linear limiting radii *vs.* linear core radii are plotted in Fig. 4. We fitted a linear trend which resulted in an equation:

$$R_{lim} = (\mathbf{6.12} \pm 0.12)\, R_{core} + (\mathbf{1.28} \pm 0.14) \qquad (7)$$

where both R_{lim} and R_{core} are in pc. The correlation coefficient was found to be **0.88**. Similar relations were obtained in studies from near IR data: Nilakshi et al. (2002) studied 38 open clusters and obtained the relation $R_{lim} = 6\, R_{core}$. It is worth noticing that for 81% of open clusters studied in this paper, the limiting and core radii were smaller than 10 and 1.5 pc, respectively.

While moving away from the Galactic Plane**,** we observed a higher fraction of open clusters with greater limiting and core radii (Fig. 5a and b). The similar conclusion was reached by Tadross et al. (2002) and Schilbach et al. (2006). **For clusters younger than 500 Myr we obtained a scale height perpendicular to the Galactic Plane of 71 pc, for oldest 238 pc (Fig 5c)**. We notice that the average age of clusters increases with a distance from the Galactic Centre **(Fig. 5d)**. After removing nine outlying objects**,** the average R_{GC} of about 9.0 kpc and for the old ones of 10.0 kpc, assuming the distance from the Galactic Centre to the Sun $R_{GC\odot} = 8.3$ kpc. We binned the distribution of individual sizes of clusters into 0.3 log (*age*) bins (Fig. 6) and noticed that the average linear sizes increase with

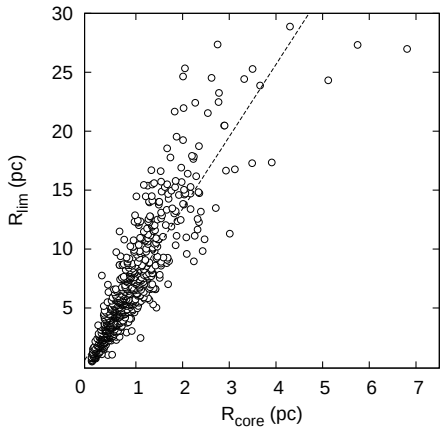

Fig. 4. The relation between the linear limiting and core radii for clusters of the sample.

age, but we observed **also** strong selection effect (see Sect. 4.2) which affects the relation between cluster sizes and their ages.

Geometrical and physical characteristics of statistically significant sample of open clusters also allowed us to check some large spatial scale properties of the system of open clusters in the Galaxy. **Our results presented in Fig. 7 reveal two regions at the Galactic longitude with a significantly diminished number of clusters what confirms results reported by Tadross et al. (2002) and Froebrich et. al (2010). A first region is located near the Galactic Centre, i.e. 60° away from it**. This is probably an effect of observational selection because at 0° we observe in the direction of the Galactic Centre where high stellar background and gas density may effectively prevent from detecting open clusters. A second region with a number of cluster smaller than average is seen at $140^\circ < l < 200^\circ$. The same effect is also observed in the distribution of stars shown by Benjamin (2008), who discovered a gap in the Perseus Spiral Arm. Froebrich et al. (2010) noted that in all-sky extinction maps by Rowles and Froebrich (2009) there is no indication of the existence of such high-extinction molecular clouds in this region. Additionally, we notice that a **second gap in the cluster distribution** is more pronounced for younger objects. Oldest clusters have orbited the Galactic Centre more times than younger ones so their distribution in the Galactic Plane is less related to the region where they have been born. Thus, this lack might be connected with a local gap in the Perseus Spiral Arm.

The concentration parameter is in a range between 0.8–1.1 for 94% of open clusters from our sample. We did not detect any relation between c and $|Z|$ or R_{GC}.

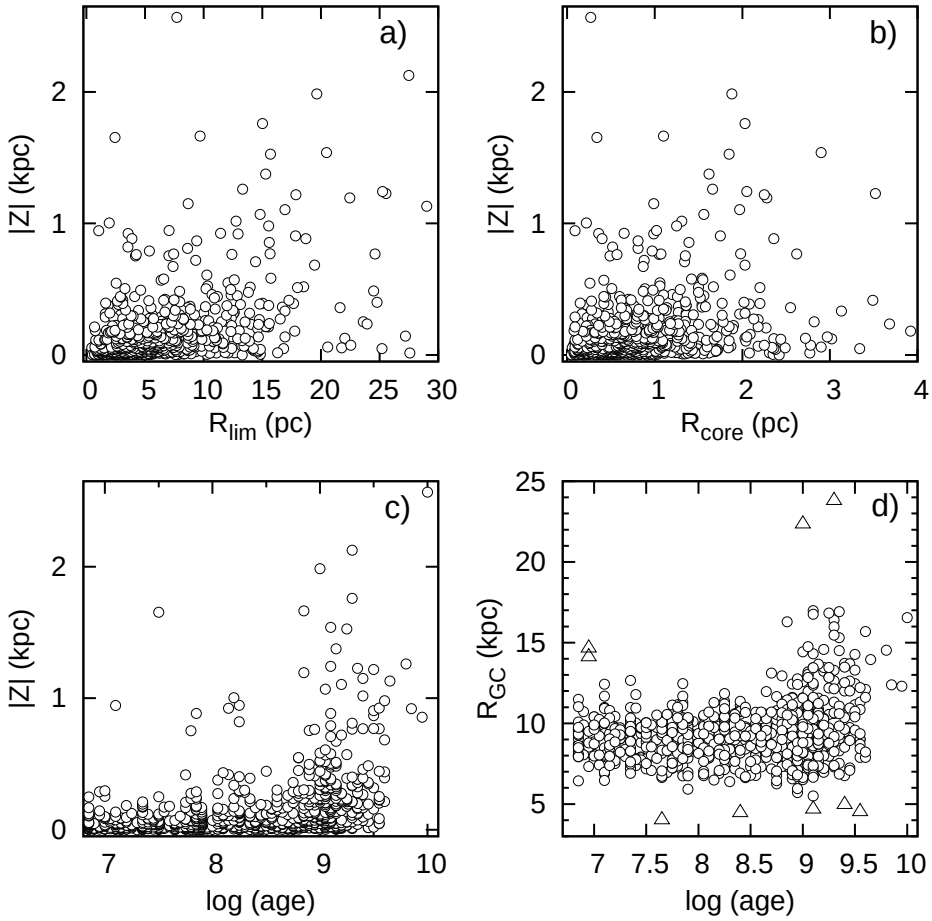

Fig. 5. a) Relation between the limiting radius in parsecs and distance from the Galactic Plane Z, assuming $Z_{\odot} = -33$ pc for the Sun. b) The same as panel a but for core radii. c) Relation between the age of open clusters and distance from the Galactic Plane Z. d) Relation between the age of open clusters and distance from the Galactic Centre R_{GC}.

4.2. Selection effects and biases

The **first** main selection effect has its source in the catalog by Dias et al. (2002), from which the list of open clusters was taken. It is a compilation of many different catalogs what makes our sample inhomogeneous. **Second is the 2MASS catalog. The maximum range of limiting magnitude of this survey is about 16.5 mag in the J band. Moreover the resolution is relatively low, what makes it difficult to study small open clusters in high density fields. Another problem is** the extinction along the line of sight. **Other bias may be** caused by extracting sources with a radius of 34 arcmin around clusters. The selection radius might introduce a bias in the cluster radius determination, in particular for larger clusters. But this is not a significant problem because the median limiting radius of the all clusters in

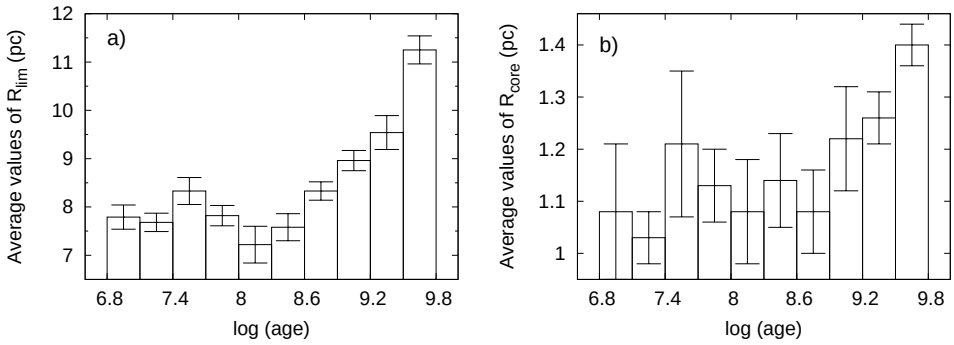

Fig. 6. *Left:* relation between the limiting radius in parsecs of open clusters and their ages. Results were presented as the average values of sizes in the particular range of the age. *Right:* relation between the core of open clusters and their ages. While constructing both diagrams we removed three clusters with log (*age*) above 9.8. We used Sturgesa's method (1926) to produce both histograms.

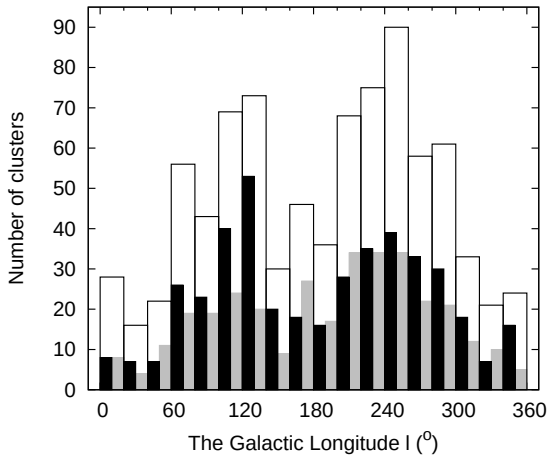

Fig. 7. Histogram showing the distribution of the clusters of our sample along the Galactic Plane. Black, grey, and white rectangles represent young ($\log(age) < 8.7$), old ($\log(age) > 8.7$), and all open clusters, respectively.

our sample is 7 arcmin.

Selection effects make **the determination of the real limiting size of clusters impossible**, so there is **a** possibility that all open clusters are bigger than our determinations, and our r_{lim} is a lower limit for cluster size.

Finally, we found important selection bias in our sample. In Fig. 8a and b we show that cluster sizes increase with distance from the Sun. For all clusters we obtained relations:

$$R_{lim}\,(\mathbf{pc}) = (\mathbf{2.080 \pm 0.038})\; d\,(\mathbf{kpc}) \qquad (8)$$

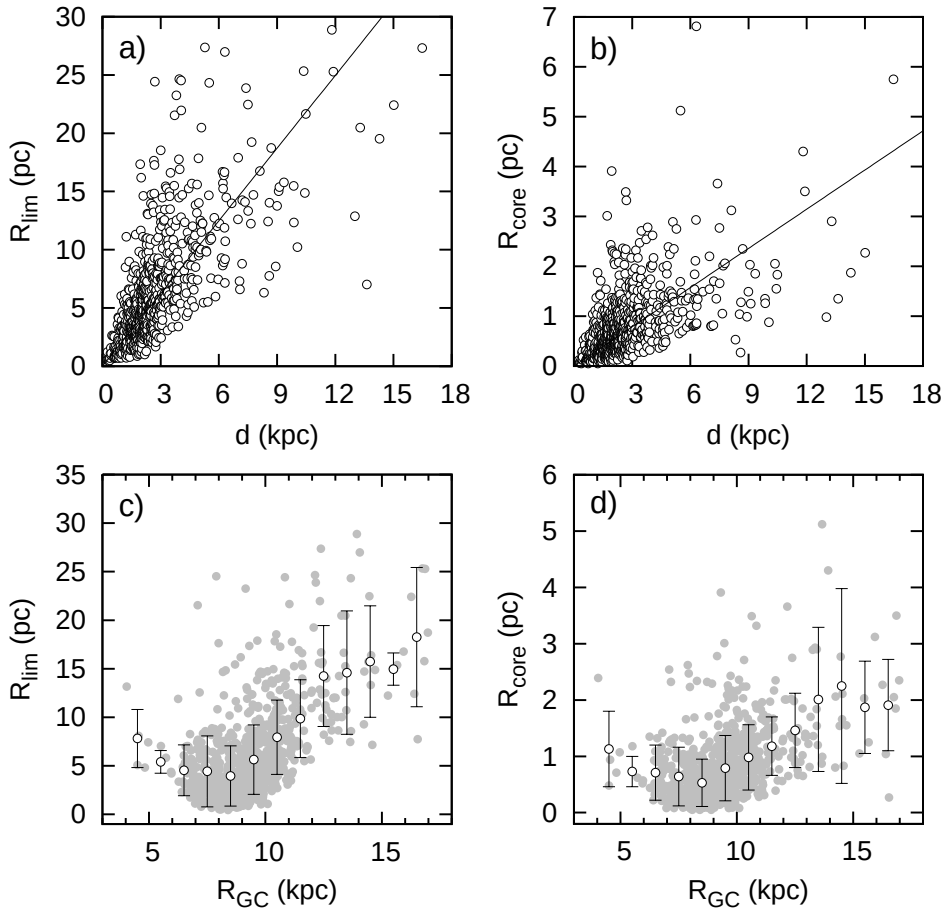

Fig. 8. a) Relation between the limiting radius and distance from the Sun. b) The same but for core radii. The black lines indicate the correlation as given in equations **9** and **10**. c) Relation between the limiting radii and the distance from the Galactic Centre R_{GC}. The Sun is located at $R_{GC_\odot} = 8.3$ kpc. Gray points represent individual measurements while black ones mean values in succeeding bins. The bin size is 1 kpc. d) The same as c but for core radii.

$$R_{core}\,(\mathbf{pc}) = (\mathbf{0.262} \pm \mathbf{0.007})\; d\,(\mathbf{kpc}) \tag{9}$$

with the correlation coefficient **0.67** and **0.47**, respectively. The same problem was encountered by Froebrich et al. (2010). This selection effect causes R_{lim} and R_{core} to increase with distance from the Galactic Centre, what is illustrated in Fig. 8c and d, respectively. Similar trend has already been observed by Lyngå (1982), van den Bergh et al. (1991), Tadross et al. (2002) and Bonatto and Bica (2010), but we argue that there is a strong selection effect in this trend. When observing distant open clusters we fail to detect smaller ones, so all samples must exhibit a lack of distant, compact open clusters. Hence our study of the evolution of cluster sizes

(in particular the limiting size) with age and position in the Galaxy are encumbered with selection effects.

5. Conclusions

The near–infrared JHK_S photometric data from the 2MASS *Point Source Catalogue* (Skrutskie et al. 2006) was used to determine structural and physical parameters of a large sample of known open clusters. The structural properties have been determined for the complete sample of 849 open clusters, while the age and distance were obtained for 754 of them.

We showed that open clusters studied in near-infrared seem to be larger than in optical bands. The same property was noticed by Sharma et al. (2006). Near IR data allow us to detect faint cluster members located far from the cluster core and are not limited by the telescope's field of view.

We obtained a different relation of $E(J-K_S)/E(B-V)$ than the one given by Schlegel et al. (1998) who obtained $E(J-K_S)/E(B-V) = \mathbf{0.520}$. Our results give $E(J-K_S)/E(B-V) = \mathbf{0.463}$. This difference translates into the error of the distance determinations of only **2.8**%. We noticed that when moving outward from the Galactic Plane and the Galactic Centre the reddening of clusters statistically decreases. The mean $E(B-V)$ for $|Z| < 0.1$ kpc is **0.68** mag, between 0.1 and 0.4 kpc is equal to **0.51** mag and for $|Z| > 0.4$ kpc is only **0.34** mag. We showed the similar trend for R_{GC}. For clusters located near the Sun's orbit and further than 8.3 kpc from the Galactic Centre, the mean $E(B-V)$ is **0.74** and **0.53** mag, respectively. This may be implied by the fact that the dust and gas density decreases, too.

For the majority of studied clusters (81%) the limiting radii was found to be smaller than 10 pc and the core radii smaller than 1.5 pc. Statistically the limiting radius is about 6–7 times larger than the core radius. We also noticed that the average cluster sizes appear to grow with a distance from the Galactic Centre and Galactic Plane. This effect has already been observed by Lyngå (1982), van den Bergh et al. (1991), Tadross et al. (2002), Schilbach et al. (2006) and Bonatto and Bica (2010). Moreover, we noticed that the average age of clusters increases with a distance from the Galactic Centre and the Galactic Plane what was shown by Janes and Phelps (1994), Friel (1995), Tadross et al. (2002) and Froebrich et al. (2010).

Open clusters, younger than 500 Myr, have a scale height of 71 pc, while older clusters 238 pc. These results are similar to Janes and Phelps (1994) who derived scale heights of 55 pc and 375 pc for young and old clusters, respectively. We found that a number of older clusters increases with the distance from the Galactic Centre. For younger clusters we obtained an average $R_{GC} = 9.0$ kpc and for the older ones – 10.0 kpc. This seems to confirm values of 8.9 and 9.4 kpc for younger and older clusters, respectively, obtained by Froebrich et al. (2010) and by Tadross et al. (2002) who found that younger clusters are concentrated at $R_{GC} < 9.5$ kpc. This

shows a difference between younger and older clusters in their location. We also notice that older clusters seem to be larger than the younger ones, what was shown by Lyngå (1982) and Tadross et al. (2002).

Moreover we found important selection effects in our sample. Cluster sizes grow with distance from the Sun, the same problem was encountered in Froebrich et al. (2010).

We observed a smaller number of clusters at the Galactic longitude range of $140^\circ < l < 200^\circ$ what is in agreement with Tadross et al. (2002) and Froebrich et al. (2010). This may reflect the structure of the Galaxy in this direction where there is a gap in the Perseus Arm (Benjamin 2008).

Acknowledgements. This research is supported by "Stypendia dla doktorantów 2008/2009 – ZPORR" SPS.IV-3040-UE/204/2009. This publication makes use of data products from the Two Micron All Sky Survey, which is a joint project of the University of Massachusetts and the Infrared Processing and Analysis Center/California Institute of Technology, funded by the National Aeronautics and Space Administration and the National Science Foundation.

REFERENCES

Benjamin, R. A. 2008, *BAAS*, **40**, 266.
van den Bergh, S., Morbey, C., & Pazder, J. 1991, *ApJ*, **375**, 594.
Bessell, Michael S. 2005, ***ARA&A***, **43**, **293**.
Bica, E. & Bonatto, C. 2005, *A&A*, **443**, 465.
Bica, E., Dutra C.M., Soares J. & Barbuy B. 2003, ***A&A***, **404**, **223**.
Cardelli, J. A., Clayton, G. C., & Mathis, J. S. 1989, *ApJ*, **345**, 245.
Dias, W. S., Alessi, B. S., Moitinho, A., & Lépine, J. R. D. 2002, *A&A*, **389**, 871.
Dutra, C. M. & Bica, E. 2001, ***A&A***, **376**, **434**.
Friel, E. D. 1995, *ARA&A*, **33**, 381.
Froebrich, D., Schmeja, S., Samuel, D., & Lucas, P. W. 2010, *MNRAS*, **409**, 1281.
Girardi, L., Bertelli, G., Bressan, A., et al. 2002, *A&A*, **391**, 195.
Janes, K. A. 1979, ***ApJS***, **39**, **135**.
Janes, K. A. & Phelps, R. L. 1994, *AJ*, **108**, 1773.
King, I. R. 1966, *AJ*, **71**, 64.
Lyngå, G. 1980, ***IAUS***, **85**, **13**.
Lyngå, G. 1982, *A&A*, **109**, 213.
Maciejewski, G. & Niedzielski, A. 2007, *A&A*, **467**, 1065.
Mighell, K. J., Rich, R. M., Shara, M., & Fall, S. M. 1996, *AJ*, **111**, 2314.
Nilakshi, Sagar, R., Pandey, A. K., & Mohan, V. 2002, *A&A*, **383**, 153.
Peterson, C. J. & King, I. R. 1975, *AJ*, **80**, 427.
Rowles, J. & Froebrich, D. 2009, *MNRAS*, **395**, 1640.
Schilbach, E., Kharchenko, N. V., Piskunov, A. E., Röser, S., & Scholz, R. 2006, *A&A*, **456**, 523.
Schlegel, D. J., Finkbeiner, D. P., & Davis, M. 1998, *ApJ*, **500**, 525.
Sharma, S., Pandey, A. K., Ogura, K., et al. 2006, *AJ*, **132**, 1669.
Skrutskie, M. F., Cutri, R. M., Stiening, R., et al. 2006, *AJ*, **131**, 1163.
Tadross, A. L., Werner, P., Osman, A., & Marie, M. 2002, *New A*, **7**, 553.

A Parameters of studied open clusters

Table 1

The list of the studied open clusters the new equatorial and galactic coordinates for epoch J2000.0, α and δ – the equatorial coordinates, l and b – the Galactic Longitude and Latitude, r_{lim} – the limiting radius (angular), r_{core} – the core radius (angular), R_{lim} – the limiting radius (linear), R_{core} – the core radius (linear), c – the concentration parameter.

Star cluster	α δ	l	b	r_{lim}	r_{core}	R_{lim}	R_{core}	c
	hhmmss ± *ddmmss*	(°)	(°)	(')	(')	(pc)	(pc)	
Berkeley 58	000013+605619	116.7498	-1.3168	11.9±0.8	2.04±0.16	9.32±1.22	1.60±0.23	0.76
Stock 18	000136+643724	117.6224	2.2666	6.0±0.4	0.37±0.03	2.17±0.27	0.14±0.02	1.20
Berkeley 104	000328+633546	117.6289	1.2194	5.2±0.5	0.51±0.04	7.39±1.20	0.73±0.10	1.01
Czernik 1	000744+612823	117.7376	-0.9571	1.7±0.2	0.26±0.03	0.88±0.16	0.14±0.02	0.81
Berkeley 1	000946+602851	117.8173	-1.9764	7.3±0.6	0.94±0.07	7.38±1.07	0.95±0.13	0.89
King 13	001019+611031	117.9946	-1.3017	15.6±1.0	2.53±0.16	13.45±1.70	2.18±0.27	0.79
Juchert-Saloran 1	001619+595758	118.5456	-2.6062	8.7±0.6	1.09±0.07	9.80±1.33	1.23±0.16	0.90
Berkeley 60	001744+605616	118.8484	-1.6665	8.4±0.8	1.10±0.08	11.01±1.80	1.44±0.20	0.88

Table 2

The list of the studied open clusters: log (*age*) – the logarithm of age, $m-M$ – the distance modulus, $E(J-K_S)$ and $E(B-V)$ – the reddening, d – the distance from the Sun, Z – a distance from the Galactic Plane, with assumption Z for the Sun $Z_\odot = -33$ pc, R_{GC} – a distance from the Galactic Centre with assumption R_{GC} for the Sun $R_{GC\odot} = 8.3$ kpc. An error for the age, m-M and reddening we assumed respectively **0.05**, 0.1 and 0.03 for more details please see the paper (Sect. 2.4.)

Star cluster	Age	m-M	$E(J-K_S)$	$E(B-V)$	d	Z	R_{GC}
	log (*age*)	(mag)	(mag)	(mag)	(kpc)	(kpc)	(kpc)
Berkeley 58	8.25	12.70	0.34	0.64	2.699±0.178	-0.062±0.004	9.815±0.077
Stock 18	8.10	11.08	0.37	0.69	1.252±0.083	0.050±0.003	8.949±0.038
Berkeley 104	8.85	13.83	0.23	0.43	4.925±0.310	0.105±0.007	11.448±0.132
Czernik 1	7.25	11.79	0.32	0.60	1.801±0.118	-0.030±0.002	9.276±0.054
Berkeley 1	9.00	13.16	0.29	0.54	3.461±0.223	-0.119±0.008	10.377±0.099
King 13	8.90	12.81	0.28	0.52	2.968±0.190	-0.067±0.004	10.041±0.086
Juchert-Saloran 1	9.05	13.64	0.43	0.80	3.894±0.266	-0.177±0.012	10.721±0.120
Berkeley 60	8.25	14.04	0.48	0.90	4.512±0.315	-0.131±0.009	11.198±0.142

[1]Full data tables available at http://www.astri.uni.torun.pl/~ gm/OCS/2mass.html

B Colour–magnitude diagrams

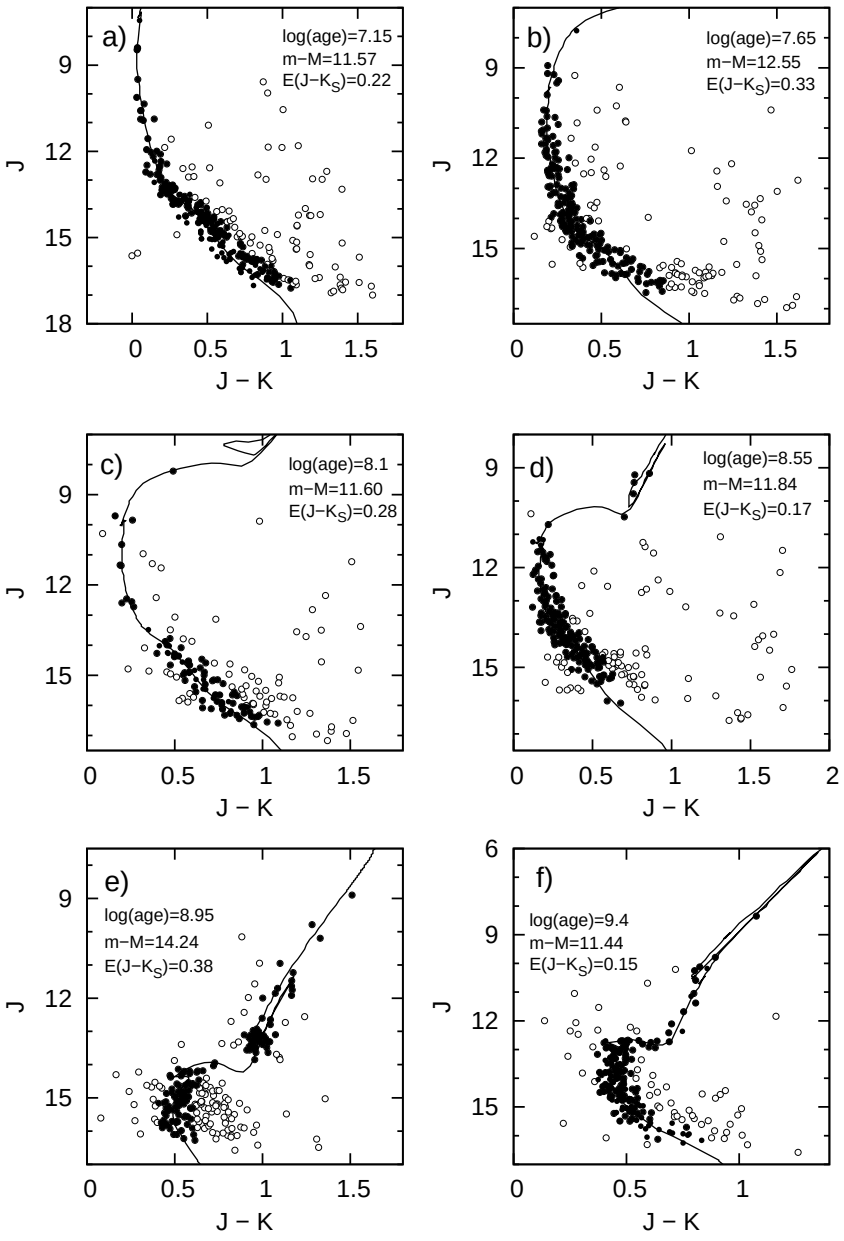

Fig. 9. Colour–magnitude diagrams after the cleaning procedure for six different open clusters. Filled circles represent stars used for fitting isochrones while open circles – stars manually removed after visual inspection. The best-fit isochrones are drawn with solid lines. a) NGC 2645 b) NGC 663 c) Markarian 50 d) Melotte 105 e) IC 166 f) NGC 6253. For more information about open clusters please see Table 1 and 2.